Key Role of the Dispersion of carbon nanotubes (CNTs) within Epoxy Networks on their ability to Release

Jannick Duchet-Rumeau, Maxime Pras, Jean-François Gérard, Luana Golanski, Guilhem Quintard, ; Jannick Duchet- Rumeau

polymers

MDPI

Article

Key Role of the Dispersion of carbon nanotubes (CNTs) within Epoxy Networks on their ability to Release

Maxime Pras[1,2], Jean-François Gérard[1], Luana Golanski[2], Guilhem Quintard[1];. Jannick Duchet-Rumeau[1*]

[1]Univ. Lyon, INSA Lyon, UMR CNRS 5223, IMP Ingénierie des Matériaux Polymères, F-69621 Villeurbanne, France

[2]LITEN, CEA-Grenoble, 17 rue des Martyrs 38054 Grenoble Cedex 09 France

*****Correspondence: Jannick.duchet@insa-lyon.fr

Received: date; Accepted: date; Published: date

Abstract: Carbon nanotubes (CNT) reinforced nanocomposites represent an unique opportunity in terms of designing advanced materials with mechanical reinforcement and electrical and thermal conductivities improvements. However, toxic effects of these composites on human health still have been studied and very soonly some regulations on CNT and on composites based on CNT will be enacted. That is why CNT releasing during nanocomposites lifecycle must be controlled. As the releasing depends on the interfacial strength that is stronger between CNT and polymer compared to CNTs in a CNTs agglomerate, two dispersion states, one poorly dispersed *versus* another well dispersed are generated and finely described. So the main aim of this study is to check if CNT dispersion state has an influence on the CNT potential releasing in the nanocomposite. To well tailor and characterize the CNT dispersion state in the polymer matrix, the electronic microscopies (SEM and TEM) but also the rheological analysis are carried out to well identify if CNTs are isolated, in bundles or in agglomerates. When the dispersion state is known and controlled, its influence on the polymerization kinetic and on mechanical properties is discussed. It appears clearly that in the case of good dispersion state, strong interfaces are generated linking the isolated nanotubes with the polymer whereas the CNT cohesion in an agglomerate seems much more weak and it does not provide any improvement to the polymer matrix. Raman spectroscopy is relevant to analyze the interfacial properties and allows the relationship with the releasing ability of nanocomposites, *i.e.* CNTs poorly dispersed in the matrix are more readily released when compared to well dispersed nanocomposites. The tribological tests confirm from released particles granulometry and observations that a CNT dispersion state sufficiently achieved in the nanocomposite avoids single CNT releasing under those solicitations.

Keywords: Carbon nanotube, epoxy networks, releasing

1. Introduction

Carbon nanotubes (CNTs) always have been very attractive nanofillers because of their remarkable properties. CNTs exhibit an extraordinary large specific surface area depending on diameter combined to an exceptionally high stiffness and electrical conductivity [1]. As a result, CNTs have a real potential for processing the polymer composites and for getting mechanical reinforcement but also thermal and electrical conductivities improvement while making the materials more lightweight [2-4]. However the toxicological effects of CNTs on human health are still under study regarding morphological similarities with asbestos and other small fibers [5-6-7]. A release of nanotubes can occur not only during the CNTs production but also during the use of manufactured nanocomposites [8]. Tailoring the releasing of isolated CNT during the nanocomposites lifecycle and especially during the different steps of handling (like friction, mechanical abrasion or breakage) is strongly required for a responsible development of these NTC nanofilled polymers materials [9-10]. Up to now, the risk caused by the exposure to CNTs has been hard to evaluate by lacking of data about the impacts on human health and the environment. Precautionary measures have been recommended to protect the workers, users and the environment. The potential release of CNTs from composite materials as a result of cutting, drilling, sanding, grinding and UV-light weathering has been investigated [11]. Most of them reported the particles generated were predominantly micron sized with protruding CNTs but generally without isolated NTCs [12-14]. Only Schlagenhauf *et al* showed the release of free-standing individual CNTs from CNTs-embedded nanocomposites in addition of abraded particles from the epoxy matrix and agglomerates of CNTs during an abrasion process [15]. Nanocomposites are processed by a wide variety of mixing protocols and include a range of formulations that can impact how CNTs are integrated and encapsulated within the composite. Kohler *et al* showed that the likelihood and form of release of nanotubes were determined by the way CNTs are incorporated into the material [16]. In order to understand the toxicological potential of handling CNT-containing composites, characterizing and quantifying the amount of free CNTs versus matrix-bound ones is relevant. A good dispersion state of the nanotubes in the matrix is required to increase the composite performances but what about the impact of this dispersion state on the CNT releasing process in the environment ? Interactions between a CNT and the surrounding polymer matrix and between CNTs in nanotubes agglomerates are significantly different. Several literature works review the different methods to evaluate and measure the interfacial stress, *i.e.* IFSS, between a CNT and a polymer matrix and between two CNTs. Even if very different values of IFSS are reported depending on the type of measurement approach, computational simulations versus experimental microdebonding tests, these ones are high are due to strong physical and chemical bonds at the CNT/polymer interface [17-21]. An average value of 100 MPa can be kept in mind against only 1 MPa for the interfacial stresses existing between two CNTs side by side (such as encountered in CNT agglomerates) which corresponds to the stress necessary to overcome Van der Waals interactions [22-24]. As a result, this study consisted in i) generating different dispersion states of CNT within an epoxy matrix from masterbatch in order to get either individually dispersed CNT or CNT agglomerates and ii) finely characterizing those dispersion states thanks to different multiscale approaches in order to well understand the impact of the nanocomposite morphology on its ability to release particules during its lifetime.

2. Materials and Methods

2.1-Materials

The epoxy prepolymer is the diglycidyl ether of Bisphenol A LY556 from Huntsman Co. (DGEBA, $\overline{n} = 0.15$). The hardener chosen the diaminodiphenylsulfone denoted as DDS from Aldrich is added with a stoichiometric ratio aminohydrogen to epoxy equal to 1. This hardener leads to a network with a high Tg equal to 220°C after curing 2 hours at 150°C and 3 hours at 220°C. The CNT used in this study are multiwall carbon nanotubes, MWNT, provided by Arkema under the form of a DGEBA-based masterbatch (25 wt% MWNT). The CNTs have a mean outer diameter of 12 nm and a mean inner diameter of 5 nm. Their length is from 100 nm to several μm (average length of about 800 nm).

2.2-Nanocomposite processing

In order to get the proper weight fraction of CNT in the nanocomposite, the masterbatch is diluted in the DGEBA prepolymer to get 1 wt% in the DGEBA prepolymer leading to 0.7 wt% of CNT in the final nanocomposite. Different processing conditions have been applied to generate varying dispersion states, *i.e.* from large MWNT agglomerates, as in the masterbatch before dispersion, to nearly individually dispersed nanotubes. Two tools with different shearing rates have been compared : i) a rotary blade Turbotest Rayneri (with a speed of rotation set at 2000 rpm) and ii) a 3 roll-mill Exakt 80E.

2.3-Characterization of the dispersion state

2.3.1.In DGEBA prepolymer-CNT suspensions

Investigating the rheological properties of nanofilled suspensions is known to be a powerful method to understand the nanofillers organization into a liquid medium such as DGEBA prepolymer. Frequency sweep tests were performed from 100 to 0.1 rad/s using an AR1000 (TA) rheometer with a cone-plate geometry in the linear viscoelastic region of DGEBA/MWNT suspensions.

2.3.2. In nanocomposites at the solid state

The morphology of nanocomposites, *i.e.* cured systems, is observed by Scanning Electronic Microscopy (SEM) using a Philips XL 20 microscope and by Transmission Electronic Microscopy (TEM) using a 1200EX Jeol microscope. Specimens for TEM observations have been prepared using ultramicrotomy at room temperature.

2.4-Cure kinetics

2.4.1.Epoxy conversion rate and activation energy of reaction

In order to determine if CNTs have an influence on the epoxy conversion rate during the polymerization of epoxy-amine reactive systems, cure kinetics were carried out during 2 hours at 150°C (first step of the curing cycle). The extent of reaction for given times was calculated from the exothermal peak of residual reaction of polycondensation, ΔHr (J/g), compared to the total heat of reaction, ΔHt (J/g). According to the Kissinger method, the activation energy of the condensation reaction can be deduced from differential scanning calorimetry experiments, DSC, at different heating rates, *i.e.* 2.5, 5, 10 and 15 $K.min^{-1}$, from 30 to 350°C in order to get a complete reaction. Calorimetric measurements have been performed on the Q20 calorimeter from TA Instruments.

2.4.2. Gelation time determination

Multifrequency time sweep tests were performed on ARES with a plate/plate geometry to determine gel times of the epoxy/amine systems with or without CNT from the isofrequency crossover point of the tan δ curves during an isothermal curing (at 150°C).

2.5-Nanocomposite characterization

2.5.1. Mechanical behavior

Flexural modulus, stress at break and toughness of nanocomposites were measured and discussed as a function of dispersion states. The flexural properties have been measured at 25°C on a 2/M device from MTS. Flexural Young's modulus and stress at break have been determined considering three points bending tests on machined samples (75 x 15 x 3 mm^3). The fracture toughness has been evaluated at 25°C in order to determine critical stress intensity factor K_{Ic} on single edge notched samples (SEN) in three points bending mode.

2.5.2. Microscopy and Raman spectroscopy to analyze the stress transfer

Nanocomposites samples were fractured into liquid nitrogen for SEM (Scanning Electronic Microscopy) fracture analysis (Philips XL 20). Plastic deformation at crack tip was also analysed using TEM (Transmission Electronic Microscopy) on a 1200EX Jeol.

Micro-Raman measurements were realized on the nanocomposites having different dispersion states under compression. The spectra for the CNT were recorded using a Jobin Yvon Raman system operating at 514 nm.

2.6- Characterization of particles release

A tribological process represented in Figure 1 and already described in a previous paper was developed in order to analyze airborne particles which were released by the nanocomposite under mechanical wear [13]. The nanomaterial is disposed in a clean glove box using a light air flow filtered with an H14 HEPA filter leading to a very low background level of nanoparticles (5–10 cm^{-3}). In order to simulate two different mechanical wear, a circular brush in steel is used to simulate abrasion and

a steel rake to simulate scratching. The normal force applied on the sample by the tool is controlled thanks to an analytical balance. A load of 50 g is applied on each sample with a speed of 1500 rotation per minute during 30 seconds of solicitation followed by 30 seconds of "rest". The 'airborne particles characterization part is composed of a particles collection device on a TEM grid (VTT filtration device), an OPC (optical particle counter) Grimm 1.109 which is spectrometer giving airborne particles granulometric measurement from 250 nm to 35 µm (optical diameter) and an ELPI (electrical low pressure impactor) which gives the airborne particles granulometric measurement from 7 nm to 10 µm (aerodynamic diameter). In this work only the ELPI granulometric results will be presented since the OPC granulometric results were not sensitive enough to provide information at the nanometric scale (lower limit at 250 nm is not appropriate to detect isolated CNT).

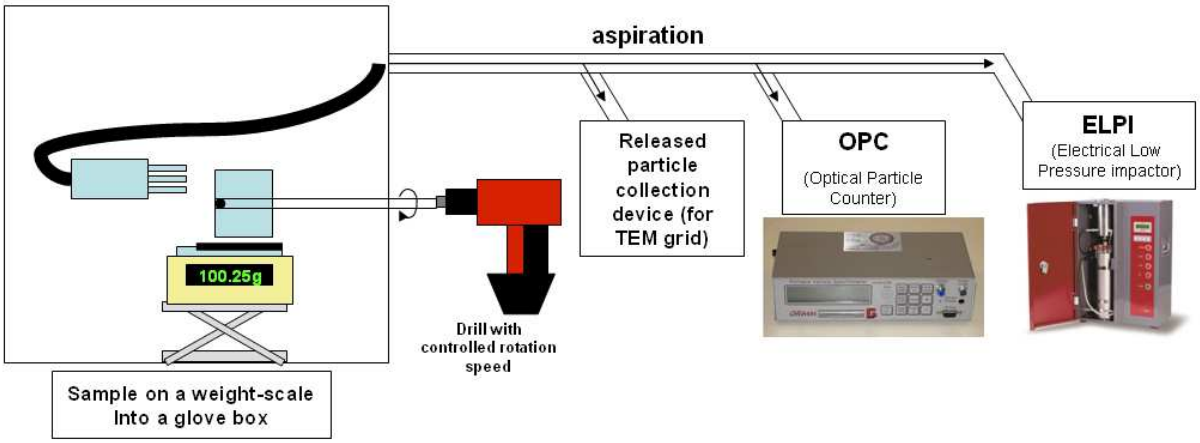

Figure 1. Representation of the wear simulation device in order to analyze airborne released particles

3-Results and discussion

3.1-Structuration of carbon nanotubes

Generating different dispersion states of CNT in a controlled way remains challenging. Tuning the processing parameters was the chosen pathway to generate extreme morphologies, *i.e.* aggregated vs dispersed. The organization of CNT within the epoxy material was studied : i) before curing, *i.e.* as the CNT-based masterbatch is dispersed in the DGEBA prepolymer and ii) after curing, *i.e.* in the solid state nanocomposites.

3.1.1. Structuration of CNT in the DGEBA-CNT suspensions

The rheology of suspensions is very sensitive to the CNT dispersion state (individually dispersed *vs* aggregated) [25-27]. In the case of a very good dispersion, the formation of a percolated network can be highlighted from the appearance of a plateau for storage modulus G' at low frequencies in the linear domain which is a signature of an elastic response at a given volume fraction. The changes in

the G′ dependence with frequency in the low frequencies region, *i.e.* the exponent of the power law f(w) decreases from 2 (liquid-like) to 0 (gel-like), could be the way to determine clearly the percolation threshold for different volume fractions of CNT. Thus, the rheological signatures of different suspensions (prepared with the same CNT weight percentage) can be compared in terms of dispersion state [25-27]. Different dispersion states of 1 wt% CNT in DGEBA prepolymer while varying dispersion tools were studied from 100 to 0.1 rad/s in dynamic mode (Figure 2). As expected the increase of the mixing time combined with the use of a high shear tool enhances the dispersion efficiency in the prepolymer. The rheological behavior of the initial DGEBA prepolymer displays a Newtonian behavior (storage modulus G′ proportional to ω^2) whereas a solid-like behavior is evidenced as the prepolymer is filled with 1 wt% of CNT, *i.e.* G′ becomes independent on the frequency at low frequencies. This evolution of G′ at low frequencies is more pronounced as the 3 roll-mill calander is used. The storage modulus values at the lowest frequency, *i.e.* at 0.1 rad/s, as well as its dependence at low frequencies according to the power law, $G' \sim \omega^{\Delta}$, are reported in Figures 2 and 3 as a function of the dispersion conditions. The same conclusions can be made from loss modulus (G′′) dependence in frequency.

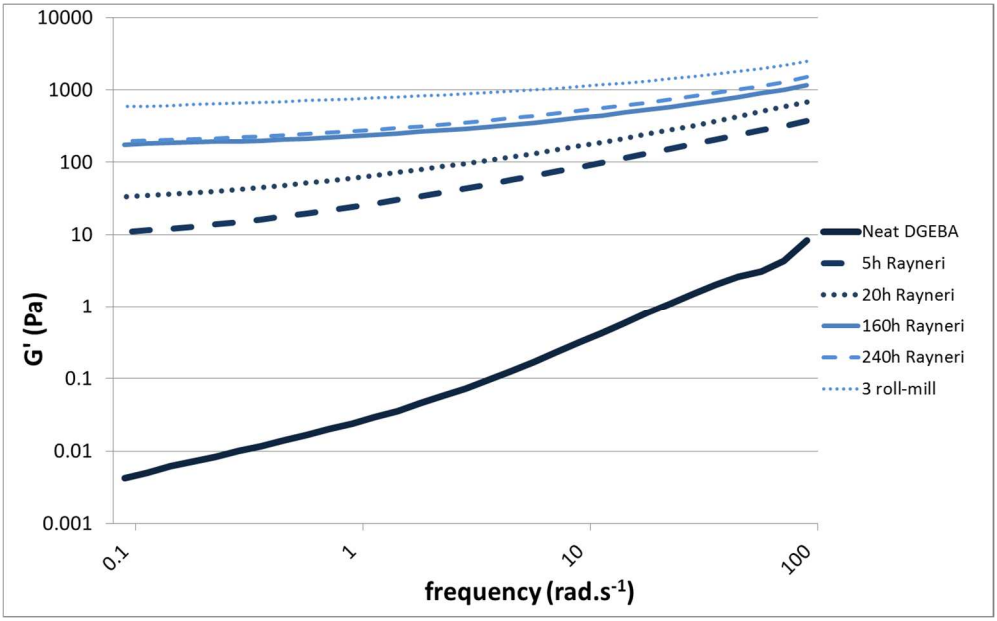

Figure 2. Evolution of storage modulus (G′) as a function of frequency, 0.1 % of dynamic strain at 25°C, for DGEBA/MWNT suspensions (1 wt%) with different mixing conditions

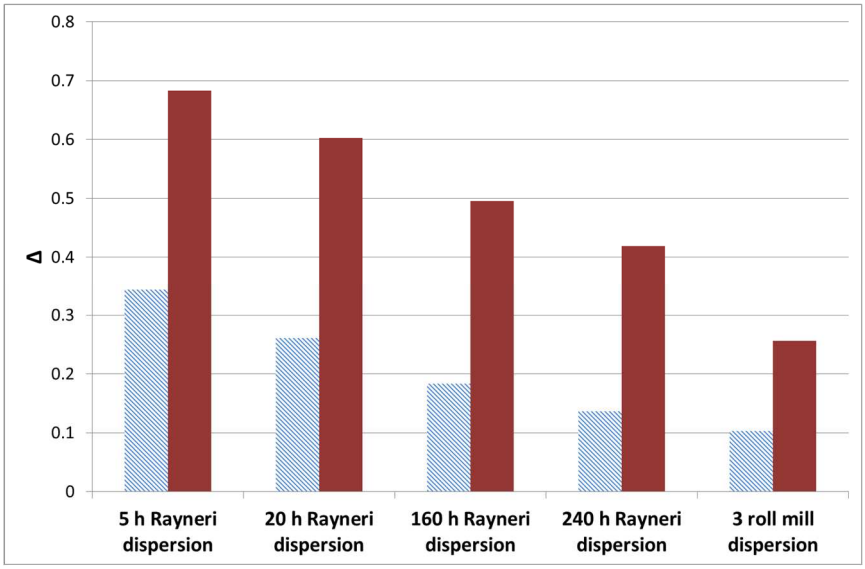

Figure 3. Δ exponent from the power law of G′ (hatched light) and G′′ (full dark) with the frequency (from 0.1 to 1 rad/s) at 25°C for DGEBA/MWNT suspensions (1 wt%) with different mixing conditions

Adding 1 % by weight of MWNT leads to a very pronounced effect on the rheological behavior of the suspension but it strongly depends on the dispersion state. The rheological signature of the suspension after 5 hours of Rayneri dispersion is completely different from the one with the best dispersion state, *i.e.* obtained using the 3 roll-mill, as G′ increases by almost 2 orders of magnitude and the exponent of the G′ dependence with frequency is almost divided by 4. Hence, the dispersion state of CNT suspension in DGEBA prepolymer, for a given content of CNT, could be quantified using rheological parameter such as dependence of storage modulus versus frequency in terminal region [28].

3.1.2. Dispersion state characterization in the final nanocomposite

The final morphology at the solid state of nanocomposites results from the freezing of the dispersion state existing on uncured DGEBA/MWNT dispersion and potential changes of the dispersion state during the 3D growing of the epoxy network during cure. Actually, the polymerization process may stabilize the dispersion state obtained before adding the amine hardener or in the opposite may modify the morphology. In order to analyze the CNT dispersion into the thermoset matrix, several methods could be used such as electron microscopies SEM and TEM which could allow to get precise information like aggregate size distributions, interparticles distances etc. For the nanocomposites having the poorest dispersion state, SEM microscopy reveals the presence of aggregates and even of agglomerates which have mean sizes around a few tens of micrometers (
Figure 4-right). The comparison between nanocomposites having different states of dispersion (
Figure 4) shows clearly the efficiency of the 3 roll-mill calander to avoid micron-size agglomerates that are observed after a dispersion of 5 hours with Rayneri rotary blade which is much less effective.

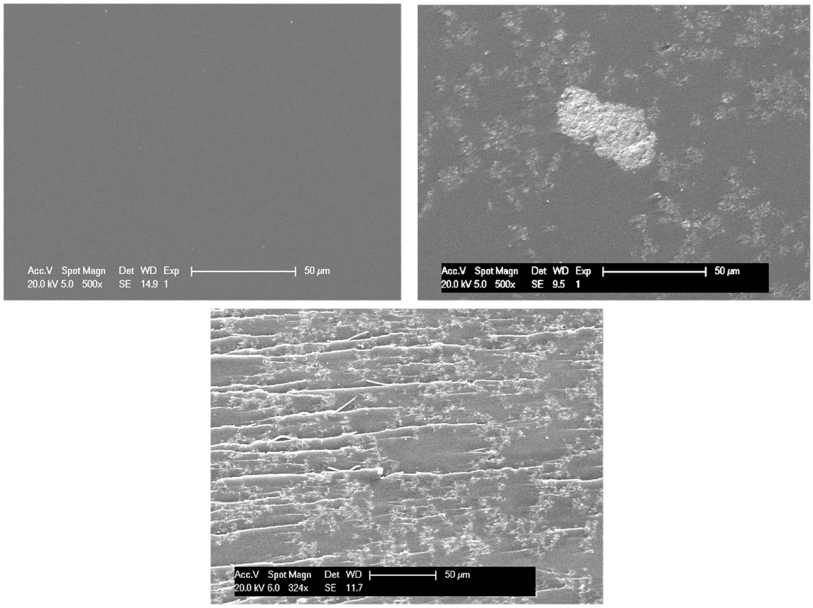

Figure 4. SEM micrograph of unfilled epoxy network (left), epoxy/DDS/MWNT nanocomposite (0.7 wt%) after a 5 h dispersion with Rayneri (right) and epoxy/DDS/MWNT nanocomposite (0.7 wt%) after a dispersion with 3 roll-mill calander (below)

As reported in a previous paper dedicated to nanoclay-based nanocomposite morphologies, the dispersion needs to be defined at different scales : from large micrometer size aggregates or agglomerates to nanoscale which is the scale of the individual nanofillers [29]. TEM (Transmission Electronic Microscopy) is a powerful method to achieve nanometric scale characterizations.

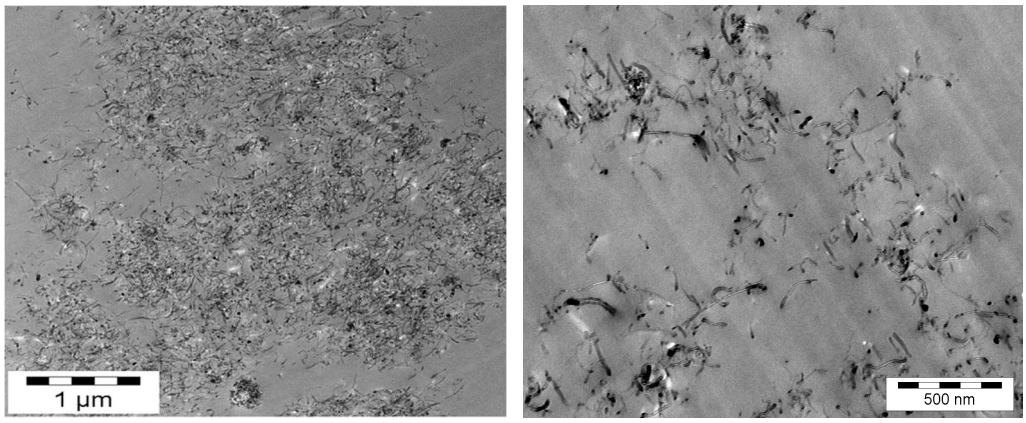

Figure 5 . TEM micrographs of epoxy/DDS/MWNT nanocomposites (0.7 wt%) after a 5h dispersion with Rayneri (left) and after a dispersion with the 3 roll-mill calander (right)

Dense CNT agglomerates can be seen in **Figure** -left corresponding to the morphology of nanocomposite with the poorest dispersion state whereas individually dispersed nanotubes got with the 3 roll-mill calander are observed in **Figure** -right corresponding to the morphology of nanocomposite with the best dispersion state. As those observations allow only a qualitative evaluation of the dispersion, quantitative analyses were performed to assess what it means the terms "poorly dispersed" and "well dispersed" CNT-based nanocomposites. An image analysis was performed in order to compute a dispersion degree DD (defined between 0 and 100; 100 meaning a

dispersion only based on individually dispersed CNT) as well as a micron size agglomerate percentage $\mu_{agglo\%}$.

$$DD = 100.P_{tot}/(P_{CNT}.N_{CNT}) \quad (1)$$

With : P_{tot} : Sum of the projected perimeters of the whole particles seen on the micrograph

P_{CNT} : Mean projected perimeter of a CNT (504 nm)

N_{CNT} : Theoretical number of CNTs on the micrographs from the particles projected area ($N_{CNT} = A_{tot}/A_{CNT}$)

A_{tot} : Sum of the projected areas of the whole particles seen on the micrograph

A_{CNT} : Mean projected area of a CNT (2880 nm²)

and

$$\mu_{agglo\%} = A_{micronic}/A_{theoretical} \quad (2)$$

With : $A_{micronic}$: Sum of the projected areas of the micronic agglomerates seen on the micrograph

$A_{theoretical}$: The theoretical area of the CNT on the micrograph from the volumic filling rate in the nanocomposite

These discriminating parameters determined for different dispersion conditions are gathered in Table 1. No pre-dispersion means have been used to break the agglomerates before adding the amino hardener.

Table 1. Dispersion degree (DD) and micron size agglomerates percentage (μagglo%) for the different DGEBA/DDS/MWNT nanocomposites (0.7 wt%) processed in different conditions (standard deviation in brackets)

	No pre-dispersion	5 h Rayneri	20 h Rayneri	160 h Rayneri	240 h Rayneri	3 roll-mill
DD	**4.9** (1.4)	**10.6** (3)	**28** (10.3)	**42** (18.7)	**44.9** (13.1)	**74.5** (15.8)
μagglo%	**73.3** (32.3)	**36.9** (20.8)	**16.1** (11.5)	**14** (16.9)	**13.4** (2.3)	**2.2** (3.6)

These discriminating parameters which are relevant to quantify the dispersion states highlight that the Rayneri mixer is very relevant to improve the dispersion for short times (DD : +100 % and **μ**agglo% : -50 % after 5 hours) but does not enhance drastically the dispersion state for very longer times of mixing. Residual micron-size agglomerates are very difficult to break and only the use of 3 roll-mill calander allows to decrease μ_{agglo}% significantly. By the combination of these analysis methods at different scales, extreme dispersion states have been generated and well characterized (with a DD from 5 to 75 and **μ**agglo% from 70 % to 2 %).

3.2-Impact of Carbon nanotubes dispersion state on the crosslinking kinetic

As montmorillonite [30, 31] or nanosilica [32], carbon nanotubes are well known to have a catalytic effect on the epoxy-amino condensation reactions by the presence of hydroxyl groups on external

297 walls [33-35]. As expected, this effect is more pronounced when the volume fraction of CNT increases
298 or when this volume fraction is well dispersed. Let's consider the effects of CNT on the condensation
299 kinetics performed on the reactive system based on DGEBA/DDS/MWNT with 0.7 % of MWNT by
300 weight.
301
302 3.2.1.Epoxy conversion rate
303
304 Thanks to isothermal DSC measurements, the extent of reaction and the reaction rate were calculated
305 (Figure 6) as proposed by Xie works [35].

306 $$\alpha = \frac{\Delta Ht}{\Delta Ht + \Delta Hr}$$

307 With : α is the advance of reaction (epoxy conversion)
308 ΔHt is the heat evolved up to a given time ($J.g^{-1}$)
309 $\Delta Ht + \Delta Hr$ is the total heat of reaction obtained from the isothermal and dynamic scan ($J.g^{-1}$)
310
311 After 2 hours at 150°C (first step of the curing cycle), the reaction kinetics for systems prepared with
312 the 3 roll-mill calander pre-dispersion step is faster compared to the unfilled reactive one. On the
313 other hand, the filled mixing without any dispersion step displays a reactivity quite similar to the
314 neat epoxy one and even slightly lower. A clear difference in the cure kinetics is highlighted during
315 the first step of the crosslinking reaction.

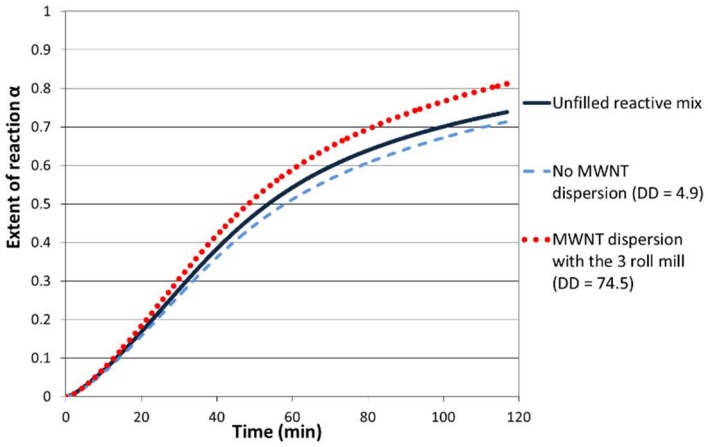

316
317 **Figure 6** . Extent of reaction (α) vs. time for a DGEBA DDS reactive system : without MWNT (continuous line)
318 and filled with MWNT (0.7% in weight) with a different dispersion state (slashed line for the poor dispersion
319 state and dotted line for the good dispersion state) at 150°C
320
321 The extent of reaction clearly depends of the MWNT dispersion state. After 2 hours at 150°C, α is
322 higher than 80 % when the 3 roll-mill was used and is equal to 71 % in the case of a poor dispersion
323 state. In this case α is even lower than the extent of reaction of the unfilled reactive system. An
324 agglomerate-based morphology induces a downturn of the reaction kinetics whereas a good
325 dispersion state has a catalytic effect on the crosslinking reaction.

It could be envisioned that some epoxy prepolymer remains confined in the MWNT agglomerates leading to a local modification of the epoxy/amine stoichiometric ratio, *i.e.* impacting reaction kinetics.

3.2.2. Activation energy of reaction in the presence of CNT

The Kissinger method [36] allows to determine the activation energy required for crosslinking reaction [37] from differential scanning calorimetry analyses (DSC) performed at different heating rates.

$$\frac{d(\ln(q/T_p^2)}{d(1/T_p)} = -\frac{Ea}{R} \quad (4)$$

With : q is the heating rate ($K.min^{-1}$)
R is the constant of gases
T_P is the temperature at the maximum of the exothermic peak (K)
Ea is the reaction activation energy ($J.mol^{-1}$)

Figure 7 gives the DSC traces evidencing the exothermic peaks of the DGEBA/DDS systems for the different heating rates.

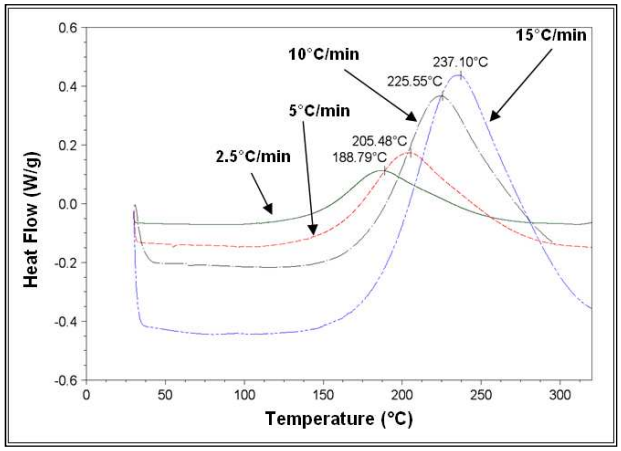

Figure 7. DSC analyses on reactive epoxy/amine (E/A) systems for different heating rates

The polymerization activation energies as a function of dispersion degrees of NTC within the epoxy/amine reactive system are reported in Table 2.

Table 2 – Polymerization activation energies of the DGEBA/DDS reactive systems filled with MWNT (0.7 % by weight) for different dispersion degrees (DD)

DD	**Ea** (kJ.mol^{-1})
Neat	71.9
4.9	71.1
10.3	70.7
28.35	69.4
47.6	69.4
74	65.9

The activation energy of the reactive system is lower in presence of MWNT whatever the dispersion state compared with the neat epoxy-amine matrix. This decrease of the activation energy is enhanced by a better quality of dispersion (up to 9% of difference between the dispersion obtained with the 3 roll-mill calander and the system without pre-dispersion).

3.2.2. Gelation time

Gelation time determination provides information about the catalytic effect of carbon nanoparticles and their influence on the changes in physical behavior of the reactive system. The formation of a chemical three-dimensional network leads to the appearance of an elastic response during polymerization. The gelation time corresponds to the transition from a liquid state to a gel, experimentally measured by chemio-rheological analyses from the crossover of the loss factor tanδ vs. time during a multi frequency time sweep. Gel times are measured at 150°C on the reactive systems based on DGEBA/DDS filled with 0.7 % of MWNT by weight tuned as a function of dispersion state.

Figure 8 shows that the finest the dispersion, the shorter the gel time. On the opposite, an agglomerated state leads to a longer gel time than one measured on the unfilled reactive system. This observation can be explained once again by the confinement of a small quantity of prepolymer within MWNT agglomerates that does not participate to the growing of the network, *i.e.* local changes of the stoichiometric ratio are generated in and close to the CNT aggregates.

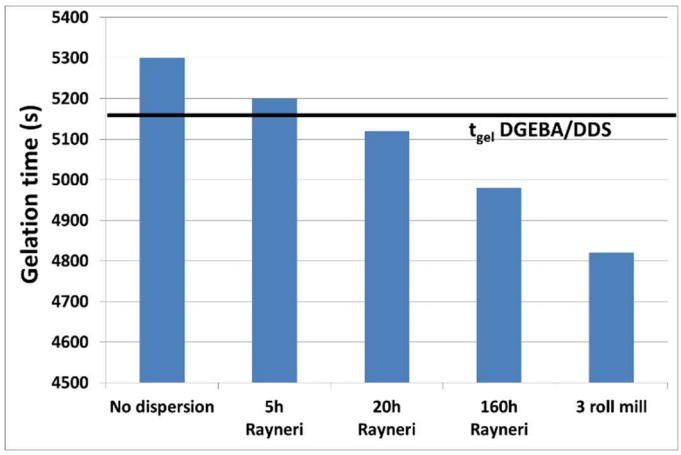

Figure 8. Gel time evolution as a function of the mixing conditions for the reactive system epoxy/amine/MWNT (0.7 wt%) at 150°C

As a conclusion, it appears that the MWNT dispersion state has a pronounced influence on the epoxy-amine system polymerization. The catalytic effect of CNT is promoted by a good dispersion state whereas a poor dispersion induces a downturn of the crosslinking reaction.

3.3-Impact of CNT dispersion on the mechanical behavior of nanocomposites

The nanocomposites having a well-defined dispersion state were selected to study their mechanical behavior. Indirect and direct analyses were carried out in order to understand the stress transfer from matrix to CNT and between CNT in the aggregates or agglomerates.

3.3.1 Macroscopic analyses

3 point bending tests carried out on nanocomposites are reported in Figure 9 and 10. As reported in the literature [12, 20, 22, 38], the mechanical properties are very sensitive to the dispersion state. Thus a poor CNT dispersion state (DD = 4.9) leads to a decrease of more than 20 % for the Young's modulus whereas the best dispersion state (DD = 74.5) leads to an increase of 10% compared to the neat epoxy network one. The stress at break is also very sensitive to the dispersion state since a decrease of 40 % with the poorest dispersion state and an increase of 35 % in the case of a good dispersion state are reported.

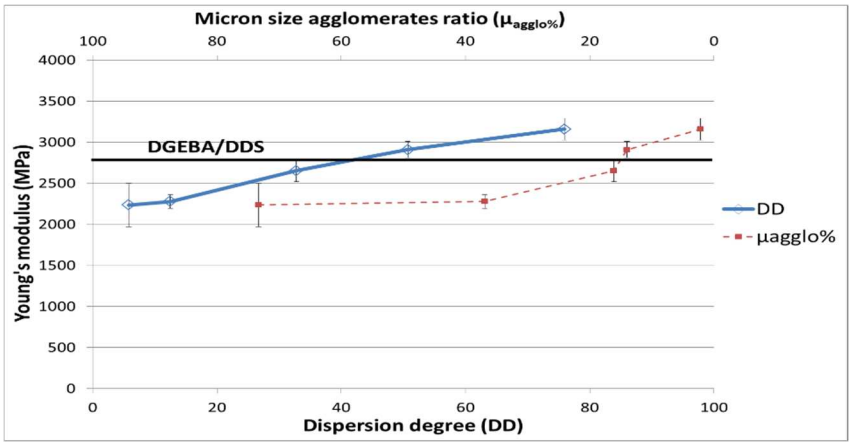

406
407
408 **Figure 9.** Young's modulus as a function of MWNT dispersion degree in the DGEBA/DDS/MWNT
409 nanocomposites (0.7 wt%)

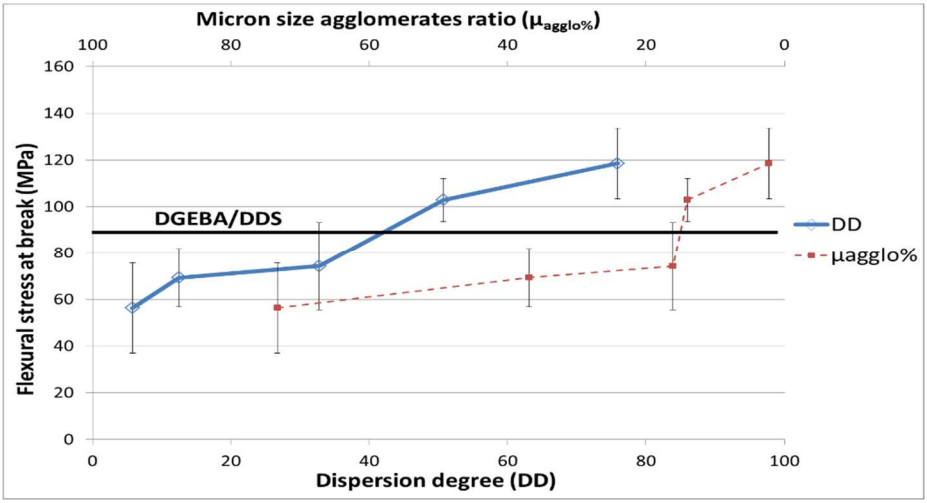

410
411
412 **Figure 10.** Flexural stress at break as a function of MWNT dispersion degree in the DGEBA/DDS/MWNT
413 nanocomposites (0.7 wt%)

414 The increase of the Young's modulus and of the flexural stress at break associated to a good
415 dispersion state of CNT can be explained by an efficient stress transfer at the CNT/polymer interface
416 as the CNT surfaces are fully in interaction with the epoxy network. On the other hand, the significant
417 decreases of these properties as the polymer matrix is filled with micronic MWNT agglomerates can
418 be explained by the poor cohesion of agglomerates that is only governed by the Van der Waals
419 interactions between MWNT. The fracture toughness of nanocomposites (
420 Figure 11) is also very sensitive to the dispersion state. K_{IC} decreases of 50 % with a poor dispersion
421 state and increases up to 22% for the best dispersion state (reached with 3 roll-mill) compared to the
422 neat epoxy network. A good dispersion state is required to take benefit from multiwall carbon
423 nanotubes on the mechanical properties of nanocomposites. Otherwise, an agglomerated
424 morphology can strongly reduce the mechanical properties of neat epoxy network. The decrease of
425 mechanical properties of nanocomposites compared to the neat network ones can be directly linked
426 to the non-polymerized DGEBA prepolymer confined in the CNT agglomerates and/or to non-
427 stoichiometric zones, as reported previously from reaction kinetics analyses.

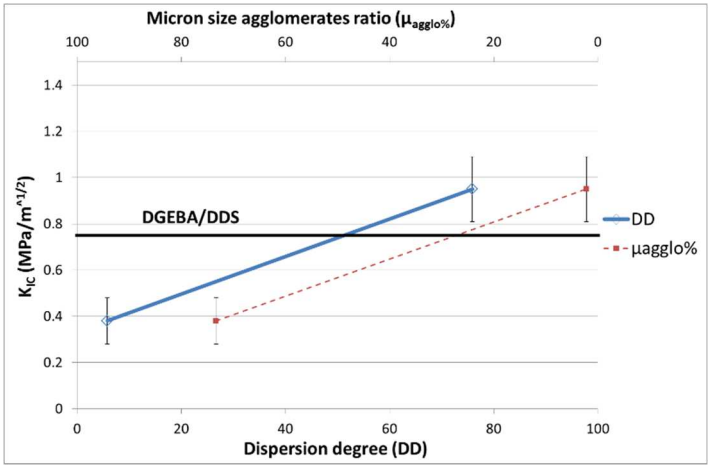

Figure 11. Fracture toughness (Critical stress intensity factor K_{IC}) as a function of the MWNT dispersion degree in the DGEBA/DDS/MWNT nanocomposites (0.7 wt%)

This reinforcing effect of CNT can be explained by the "crack-front pinning" process at the crack tip [38]. In such a process, the crack-front length increases as the crack meets rigid inclusions. As a consequence, this effect is magnified as the number of obstacles increases, *i.e.* in the case of a good dispersion state. If the MWNT are agglomerated, the number of objects decreases and their cohesion being weak (Van der Waals interactions), secondary cracks are generated.

As a conclusion, it appears that as a small amount of MWNT is well dispersed in the matrix, the mechanical properties are significantly improved compared to the unfilled polymer but they can be seriously affected if the dispersion state is not good enough. In the first case, these are the CNT/polymer interactions which govern the behavior of well-dispersed CNT-based nanocomposites whereas in the second case, this is the level of interaction between CNT that governs the behavior of poorly dispersed CNT-based nanocomposites.

3.3.2. Analysis of interfacial interactions CNT/CNT vs CNT/matrix

Interfacial interactions with CNT can be also analyzed more locally from scanning electronic microscopy (SEM) and transmission electronic microscopy (TEM) on fracture surfaces.

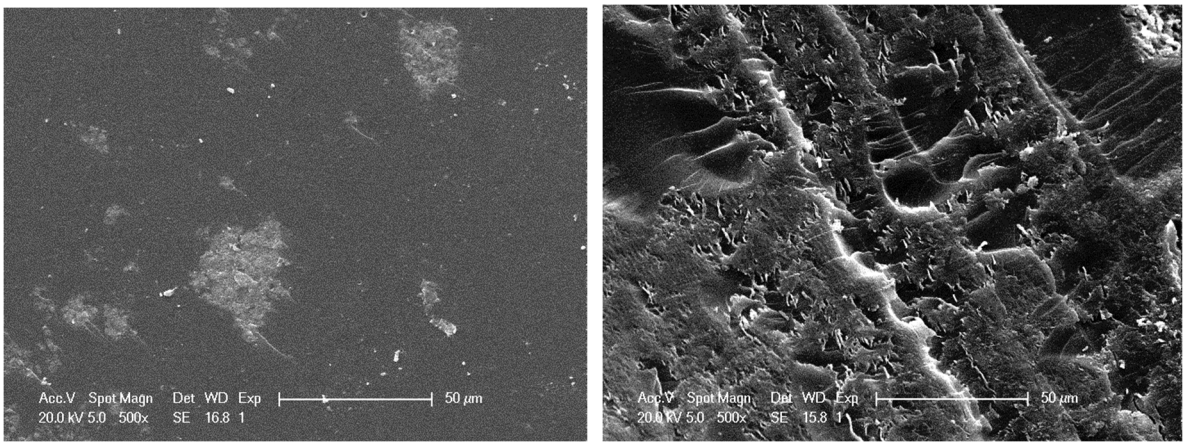

Figure 12. SEM Analysis on fractured surfaces of DGEBA/DDS/MWNT nanocomposites (0.7 wt%) with a poor dispersion state, DD = 4.9 (left) and with a good dispersion state, DD = 74.5 (right)

Epoxy networks typically exhibit a brittle fracture which can be characterized by a resulting mirror-like fracture surface. The presence of MWNT aggregated under the form of agglomerates does not modify so much the fracture surface of poorly dispersed CNT-based nanocomposites (Figure 12-left). On the other hand, the toughening effect of well dispersed MWNT is clearly shown in SEM picture (Figure 12-right). During failure, carbon nanotubes that are well wetted by the epoxy matrix induce huge plastic deformation. As a consequence, the fracture toughness increases. The roughness of the fracture surface and the presence of crack pinning are signatures of good interactions between MWNT and epoxy matrix.

In order to go further into the investigations of fracture mechanisms, TEM micrographs were realized on crack ends for the different materials (Figures 13).

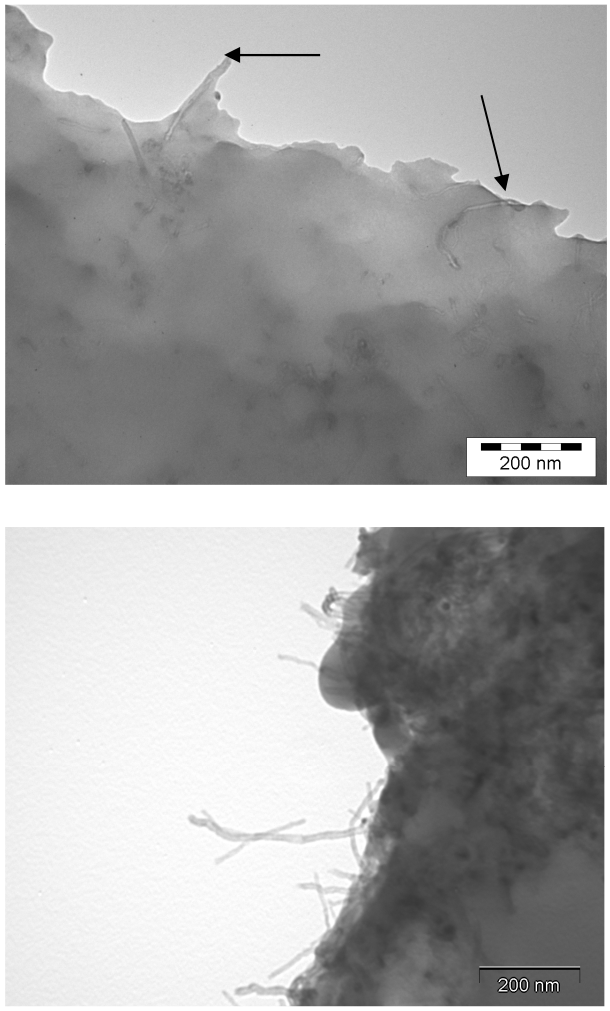

Figure 13. TEM micrographs on the fracture surfaces of DGEBA/DDS/MWNT nanocomposites (0.7 wt%). above) after dispersion using a 3 roll-mill calander, below) without pre-dispersion

Individually dispersed CNT embedded in polymer matrix are clearly observed on fracture surfaces of nanocomposite with a good dispersion state which is the signature of a good wetting (Figure 13-above) and a strong interfacial adhesion. The rough fracture profile confirms the crack-front pinning effect leading to the increase of the fracture toughness of the nanocomposite. On the other side, for the poorly dispersed CNT-based nanocomposite (Figure 13 -below), MWNT are pull-out from the polymer showing that they are not embedded by polymer matrix. The fracture surface is smooth and regular even if the crack front meets a MWNT agglomerate. Its propagation front does not seem be affected and stays straight (no toughening effect).

From those electron microscopy observations, the interactions between CNT/CNT (in agglomerates) and CNT/polymer appear clearly different, *i.e.* isolated CNT will require more energy to be extracted from surrounding polymer than ones confined in an agglomerate.

Another experimental method to measure the level of the interaction between a CNT and the polymer matrix is the micro-Raman spectroscopy. Previous works showed that the Raman spectra of carbon

fibers were sensitive to the stresses induced in the fibers along their axis [39-40]. Thus the stress transfer between polymer matrix and CNT can be assessed by considering the shift of G′ band (2,700 cm^{-1}) in the nanocomposite submitted to a compression or traction load (
Figure 14).

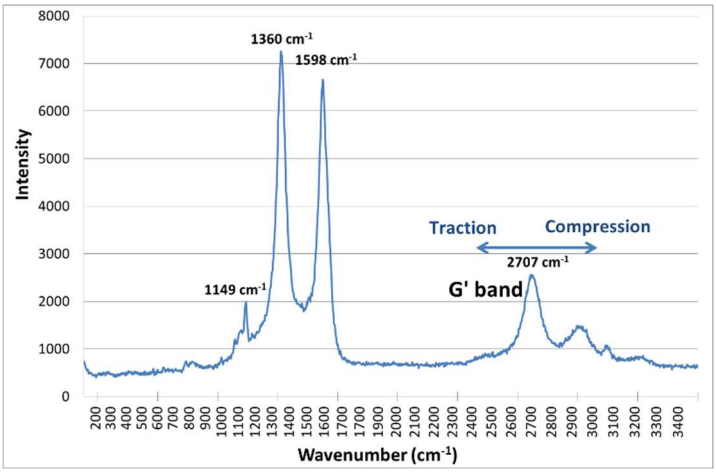

Figure 14. Raman spectrum of a MWNT-based agglomerate in DGEBA/DDS/MWNT nanocomposite (0.7 wt%, DD = 4.9)

Nanocomposites with very different dispersion states were placed under compression (1 % and 2 % of strain) and the G′ band location was followed as a function of the MWNT dispersion state (as shown in Figure 15).

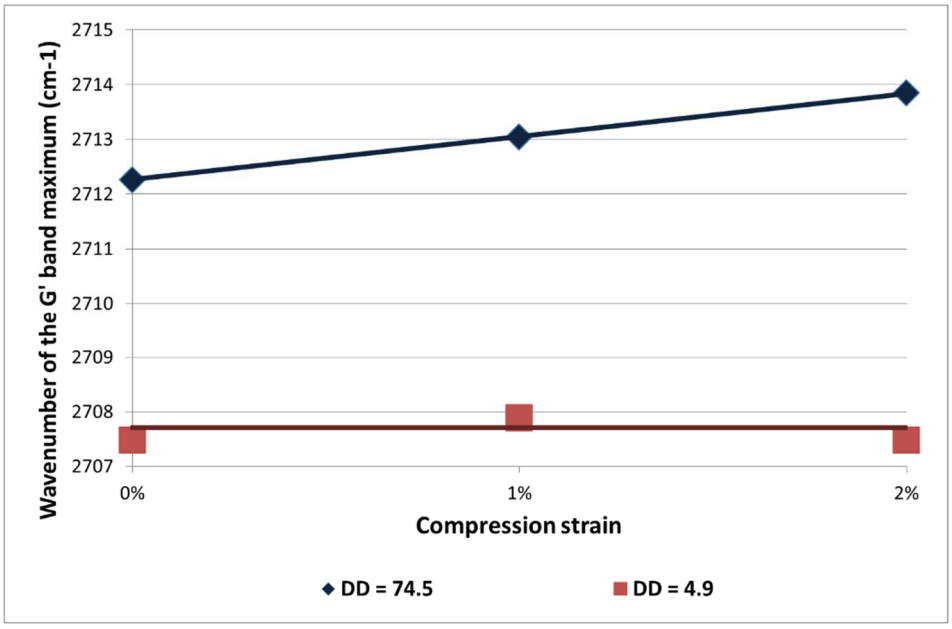

Figure 15. G′ band shift as a function of the compression strain of DGEBA/DDS/MWNT nanocomposite (0.7 wt%) and of two different dispersion states (DD=4.9 and DD=74.5)

In case of well-dispersed CNT based nanocomposite under compression, a slight shift of the G' band is observed which means that MWNTs sustain compression thanks to a good stress transfer. In the case of nanocomposite with poorly dispersed CNT, no shift of the G' band is observed whatever the strain applied to the nanocomposite. MWNTs in agglomerates probably tend to be reorganized under the matrix deformation and only few CNTs sustain compression. Nevertheless, let's note that the G' band location in both extreme dispersions is very different even without applying compression. This can be explained by the polymer shrinking during the crosslinking applying an additional compression on individually dispersed MWNT.

3.4-Impact of CNT dispersion on the potential release ability

Let's consider now the effect of the dispersion of fillers on the potential release ability during the nanocomposite life. The analysis of released particles investigated after simulating the wear undertaken by the material by using two tools either a brush or a rake is reported under form of size distribution in Figure 16 and 17. A releasing of ultrathin particles can be noted with a maximum diameter lower than 100 nm. The tool used has a non negligible influence on the releasing. The rake allows to release a higher concentration of nanoparticles (22600 cm^{-3}) with a much lower diameter (7-28 nm) in comparison with the brush (6000 cm^{-3}). This may be explained by the friction coefficient that is higher with the rake than with the brush applying an higher equivalent tensile stress from the Von Mises yield criterion. The hardness of material has also an influence on the stress applied by the tool on the sample and consequently on the releasing. The stiffness and the hardness of the glassy epoxy networks is prone to generate more particles with lower size (Wohlleben *et al* [41]).

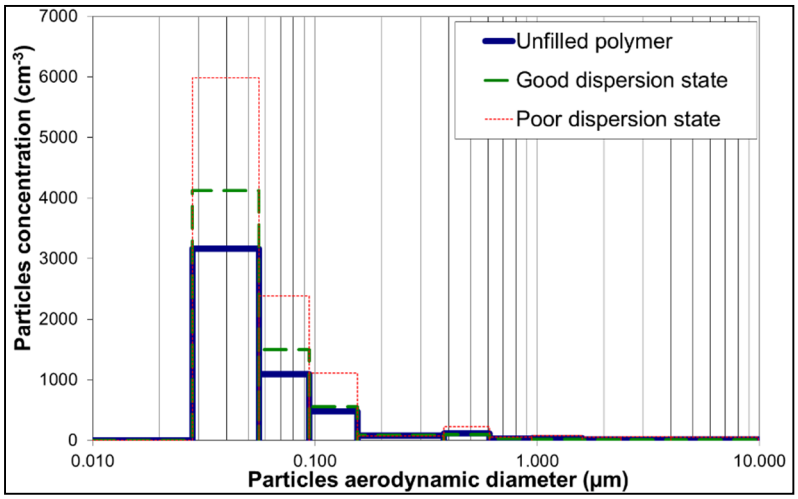

Figure 16. Granulometric distribution of released particles during the use of the steel brush on DGEBA/DDS samples (ELPI data)

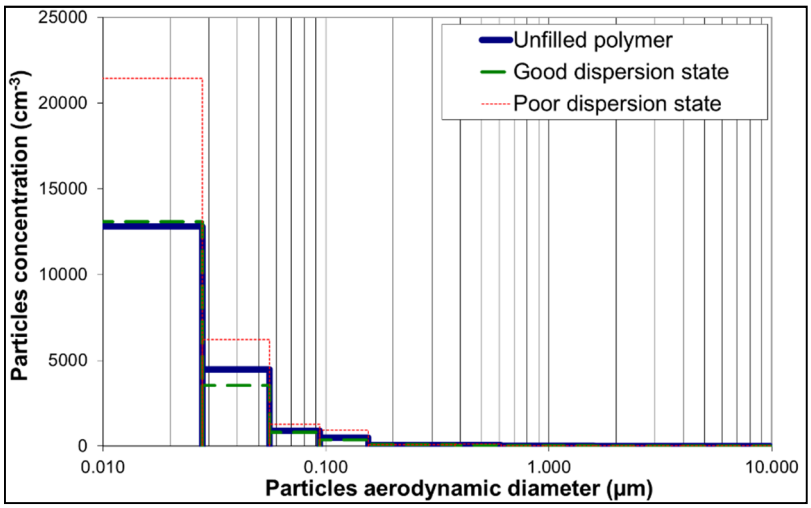

Figure 17. Granulometric distribution of released particles during the use of the steel rake on DGEBA/DDS samples (ELPI data)

At the end, the dispersion state is a significant parameter on the granulometry of released particles. The nanocomposite with a bad dispersion releases much more nanofillers (between 50 and 70% fillers with the lowest diameters) than well dispersed or unfilled ones that display the same granulometric profile. The aggregates or agglomerates behave as defects favoring the crack propagation and initiation within the nanocomposite. Under the crack effect, the particles are released out of aggregates where the NTC are embedded into confined DGEBA prepolymer. Only aggregated particles with protruding fibers are observed in TEM picture reported in Figure 18 whereas free-standing CNTs were not observed.

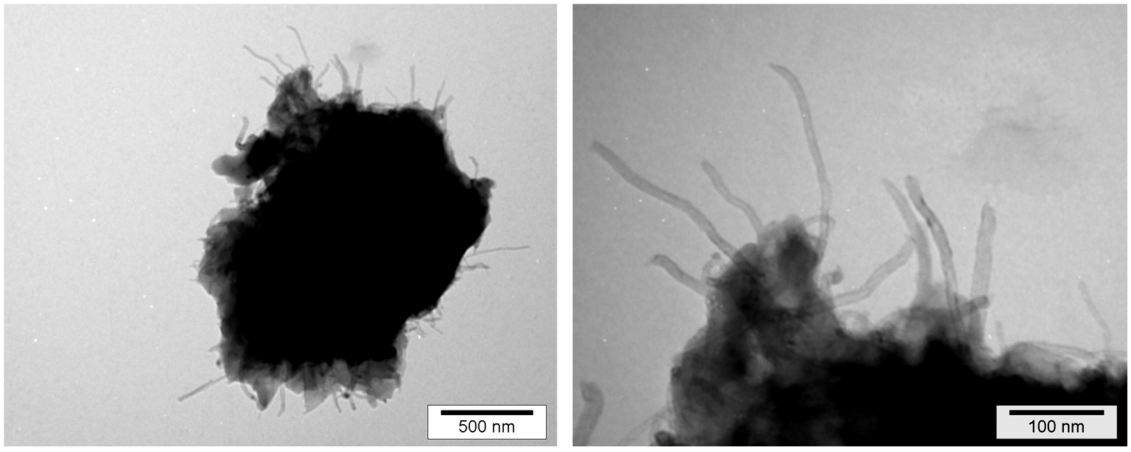

Figure 18. Released Particule after wear of DGEBA/DDS/MWNT (0.7 wt%) nanocomposite with a bad dispersion, DD = 4,9.

4-Conclusion

This paper aims at generating different dispersion states but in a controlled way of carbon nanotubes into an epoxy-amine network. Two extreme morphologies are designed by varying the dispersion tools, one with micron size agglomerates of aggregated carbon nanotubes characterized by a high micron size agglomerates percentage and another one with individual carbon nanotubes embedded into epoxy matrix, characterized by a high dispersion degree (DD). The dispersion state of carbon

nanotubes has an outstanding effect on the network build up : the gelation is catalyzed and the conversion is enhanced when the carbon nanotubes are well dispersed. In the other case, epoxy prepolymer can be confined into the carbon nanotubes aggregates locally modifying the epoxy – amine stoichiometry preventing or delaying a total conversion. A well dispersed morphology is the key architecture to reinforce the mechanical resistance of nanocomposite. Well embedded in the surrounding polymer, the carbon nanotubes ensure a good load transfer towards the matrix. On the contrary, a poor dispersion state with micron size CNT agglomerates has quite no influence on the crack direction. If the crack front founds agglomerate on its path it just goes through considering the weak agglomerate cohesion. There is no strong load transfer between CNT in agglomerate and the mechanical properties of composites containing micronic agglomerates of MWNT can be much lower than the initial properties of the unfilled polymer. After showing the huge influence of the NTC dispersion on the polymerization mechanisms at macromolecular scale and on the macroscopic behavior of nanocomposites, these works established a link between the nanocomposites morphology and the potential release of carbon nanotubes during the nanocomposite life. We checked experimentally that less energy is required to extract a CNT from an agglomerate than to extract a CNT individually dispersed in the polymer matrix.

References

[1]. Iijima S., Helical microtubules of graphitic carbon. *Nature* **1991**, *354(6348)*, 56-58.

[2]. Gojny, F.H., Wichmann, M.H.G., Fiedler, B., Schulte, K. Influence of different carbon nanotubes on the mechanical properties of epoxy matrix composites-A comparative study. *Composites Science and Technology* **2005,** *65*, 2300-2313.

[3] Ma, P.C., Siddiqui, N.A., Marom, G., Kim, J.K. Dispersion and functionalization of carbon nanotubes for polymer-based nanocomposites: a review. *Composites: Part A* **2010**, *41*, 1345-1367

[4]. Song Y. S., Youn, J.R. Influence of dispersion states of carbon nanotubes on physical properties of epoxy nanocomposites. *Carbon* **2005**, *43(7)*, 1378-1385.

[5]. Donaldson, K., Aitken, R., Tran, L., Stone, V., Duffin, R., Forrest, G., Alexander, A. Carbon nanotubes : A review of their properties in relation to pulmonary toxicology and workplace safety. *Toxicological Sciences* **2006**, *92(1)*, 5-22.

[6]. Cheng, C., Müller K.H., Skepper, J.N., Midgley, P.A., Welland, M.E., Porter, A.E. Toxicity and imaging of multi-walled carbon nanotubes in human macrophage cells. *Biomaterials* **2009**, *30(25)*, 4152-4160.

[7] Francis, A.P., Devasena, T. Toxicity of carbon nanotubes : a review. Toxicology and industrial health 2018, 34(3), 200-210

[8] Köhler, A.R., Som, C., Helland, A., Gottschalk, F. Studying the potential release of carbon nanotubes throughout the application life cycle. Journal of cleaner Production 2008, 16(8-9), 927-937

[9] Nowacka,B., Davidb, R.M., Fissanc, H., Morrisd, H., Shatkine, J.A.; Stintzf, M., Zeppg, R., Brouwerh, D. Potential release scenarios for carbon nanotubes used in composites *Environment International* **2013** 59, 1-11

[10] Petersen, E.J. Liwen, Z., Mattison, N.T., O'Carroll, D.M., Whelton, A.J., Tinh Nguyen, N.U., Huang, Q., Henry,.T.B., Holbrook, D., Chen, K.L. Potential Release Pathways, Environmental Fate, And Ecological Risks of Carbon Nanotubes. *Environ. Sci. Technol.* **2011** 45, 9837–9856

[11] Petersen, E.J., Lam, T., , J.M., Scott, K.C., Long, B.D., Stanley, D., Sharma, R., Liddle, J.A., Pellegrin, B., Nguyen, T. Methods to assess the impact of UV irradiation on the surface chemistry and structure of multiwall carbon nanotube epoxy nanocomposites. *Carbon* **2014**, 69, 194-205

[12] Kovochich, M., Fung, C.C.D, Avanasi, R., Madl, A.K. Review of techniques and studies characterizing the release of carabon nanotubes from nanocomposites : Implications for exposure and human health risk assessment. *Journal of Exposure Science and Environmental Epidemiology* **2017**, 1-13

[13] Golanski, L., Guiot, A., Pras, M., Malarde, M., Tardif, F. Release-ability of nanofillers from different nanomaterials (toward the acceptability of nanoproduct). *Journal of Nanoparticules Resarch* **2012**, *14* (962), 1-9

[14] Ogura, I., Kotake, M., Shigeta, M., Uejima, M., Saito, K., Hashimoto, N., Kishimoto Potential release of carbon nanotubes from their composites during grinding Journal of Physics : Conference Series 429 (2013)

[15] Schlagenhauf, L., Chu, B.T.T, Buha, J., Nüesch, F., Wang, J. Release of carbon nanotubes from an epoxy-based nanocomposite during an abrasion process. *Environmental Science & Technology* **2012**, *46*, 7366-7372.

[16] Köhler A.R., Som C., Helland A., Gottschalk, F. Studying the potential release of carbon nanotubes throughout the application life cycle. *Journal of cleaner Production* **2008**, *16*, 927-937.

[17]. Barber A. H., Cohen, S.R., Wagner, H.D. Measurement of carbon nanotube--polymer interfacial strength. *Applied Physics Letters* **2003**, *82(23)*, 4140-4142.

[18]. Frankland S. J. V., Caglar, A., Brenner, D.W., Griebel, M. Molecular simulation of the influence of chemical cross-links on the shear strength of carbon nanotube-polymer interfaces. *Journal of Physical Chemistry B* **2002**, *106(12)*, 3046-3048.

[19]. Xu X., Thwe, M.M., Shearwood, C., Liao, K. Mechanical properties and interfacial characteristics of carbon-nanotube-reinforced epoxy thin films, *Applied Physics Letters* **2002**, *81(15)*, 2833-2835.

[20]. Wagner H. D., Nanotube-polymer adhesion: a mechanics approach. *Chemical Physics Letters* **2002**, *361(1-2)*, 57-61.

[21]. Duncan R. K., Chen, X.G., Bult, J.B., Brinson, L.C., Schadler, L.S. Measurement of the critical aspect ratio and interfacial shear strength in MWNT/polymer composites. *Composites Science and Technology* **2010**, *70(4)*, 599-605.

[22]. Kelly B. T., Physics of graphite, *Applied Science Publishers*, London, **1981**, *114* (1).

[23]. Suhr J., Korathar, N., Keblinski, P., Ajayan, P. Viscoelasticity in carbon nanotube composites, *Nature Materials* **2005**, *4(2)*, 134-137.

[24]. Yu M. F., Yakobson, B.I., Ruoff, R.S., Controlled Sliding and Pullout of Nested Shells in Individual Multiwalled Carbon Nanotubes. *The Journal of Physical Chemistry B* **2000**, *104(37)*, 8764-8767.

[25]. Fan Z., Advani, S.G. Rheology of multiwall carbon nanotube suspensions. *Journal of Rheology* **2007**, 51 (4), 585-604.

[26]. Ma A., Chinesta, F., Mackley, M., Ammar, A., The rheological modelling of carbon nanotube (CNT) suspensions in steady shear flows. *International Journal of Material Forming* **2008**, *1(2)*, 83-88.

[27]. Li J., Ma, P.C., Chow, W.S., To, C.K., Tang, B.Z. Correlations between Percolation Threshold, Dispersion State, and Aspect Ratio of Carbon Nanotubes. *Advanced Functional Materials* **2007**, *17(16)*, 3207-3215.

[28]. Le Pluart, L. ; Duchet, J. ; Sautereau, H. ; Halley, P. ; Gérard, J.F. Rheological properties of organoclay suspensions in epoxy network precursors. *Appl. Clay Sci.* **2004**, *25 (3-5)*, 207-219.

642 [29] Vermogen A., Masenelli-Varlot, K., Seguela, R., Boucard, S., Prele, P., Duchet-Rumeau, J. Evaluation
643 of the structure and dispersion in polymer-layered silicate nanocomposites. *Macromolecules* **2005**,
644 *38(23)*, 9661-9669.
645 [30] Le Pluart, L.; Duchet, J.; Sautereau, H Epoxy /Montmorillonite nanocomposites : influence of
646 organophilic treatment on reactivity, morphology and fracture properties. *Polymer* **2005**, *46(26)*,
647 12267-12278
648 [31]. Wang M., Pinnavaia, T.J., Clay-Polymer Nanocomposites Formed from Acidic Derivatives of
649 Montmorillonite and an Epoxy Resin. *Chemistry of Materials* **1994**, 6(4), 468-474.
650 [32]. Altmann N., Halley, P.J., Cooper-White, J., Lange, J. The effects of silica fillers on the gelation and
651 vitrification of highly filled epoxy-amine thermosets. *Macromolecular Symposia* **2001**, 169(1), 171-177.
652 [33]. Wu J., Chung, D. Calorimetric study of the effect of carbon fillers on the curing of epoxy, *Carbon* **2004**,
653 42(14), 3039-3042.
654 [34]. Tao K., Yang, S., Grunlan, J.C., Kim, Y.S., Dang, B., Deng, Y., Thomas, R.L., Wilson, B.L., Wei, X
655 Effects of carbon nanotube fillers on the curing processes of epoxy resin-based composites. *Journal of*
656 *Applied Polymer Science* **2006**, 102, (6), 5248-5254.
657 [35]. Xie H., Liu, B., Yuan, Z., Shen, J., Cheng, R., Cure kinetics of carbon nanotube/tetrafunctional epoxy
658 nanocomposites by isothermal differential scanning calorimetry. *Journal of Polymer Science Part B :*
659 *Polymer Physics* **2004**, *42(20)*, 3701-3712.
660 [36]. Kissinger H. E., Reaction Kinetics in Differential Thermal Analysis. *Analytical Chemistry* **1957**, 29(11),
661 1702-1706.
662 [37]. Hayaty M., Hosain Beheshty M., Esfandeh, M. Cure kinetics of a glass/epoxy prepreg by dynamic
663 differential scanning calorimetry. Journal of Applied Polymer Science 2011, 120(1), 62-69.
664 [38]. Paiva M. C., Zhou, B., Fernando, K.A.S., Lin, Y Mechanical and morphological characterization of
665 polymer-carbon nanocomposites from functionalized carbon nanotubes. *Carbon* **2004**, 42(14), 2849-
666 2854.
667 [39]. Galiotis C., Batchelder, D.N. Strain dependences of the first- and second-order Raman spectra of
668 carbon fibres. *Journal of Materials Science Letters* **1988**, 7(5).
669 [40]. Lachman N., Bartholome, C., Miaudet, P., Maugey, M., Poulin, P., Wagner, H.D., Raman Response of
670 Carbon Nanotube/PVA Fibers under Strain. *The Journal of Physical Chemistry C* **2009**, 113(12), 4751-
671 4754.
672 [41] Wohlleben W., Mertler, M., Brill, S., Meier, M., On the Lifecycle of Nanocomposites: Comparing
673 Released Fragments and their In-Vivo Hazards from Three Release Mechanisms and Four
674 Nanocomposites. Small **2011**, 7(16), 2384-2395.
675
676

677